

Supporting Information

**Impedimetric Detection of 2,4,6-Trinitrotoluene
Using Surface-Functionalized Halloysite Nanotubes**

Supak Pattaweepaiboon¹, Varuntorn Pimpakoon¹, Nattida Phongzithiganna^{1,2},

Weekit Sirisaksoontorn^{1,2}, Kannika Jeamjumnunja^{1,2,}, and Chaiya Prasittichai^{1,2,*}*

¹Department of Chemistry, Faculty of Science, Kasetsart University, Bangkok 10900, Thailand

²Center of Excellence for Innovation in Chemistry, Faculty of Science, Kasetsart University,
Bangkok 10900, Thailand

Table S1. Positions and assignments of the FTIR bands presented in the spectra of HNTs and HA.

Wavenumber (cm ⁻¹)		Assignments
HNTs	HA	
3695	3695	O–H stretching of outer-surface hydroxyl groups
3622	3622	O–H stretching of inner hydroxyl groups
–	3456	N–H stretching
–	2932	C–H ₂ symmetric stretching
1651	1649	O–H deformation of water
–	1568	deformation (scissoring) of N–H ₂
–	1487	deformation (scissoring) of C–H ₂
1120	1118	perpendicular Si–O stretching
1024	1026	in-plane Si–O stretching
908	908	O–H deformation of inner hydroxyl groups
793	793	Si–O symmetric stretching
752	750	perpendicular Si–O stretching
681	685	perpendicular Si–O stretching
525	527	deformation of Al–O–Si
460	463	deformation of Si–O–Si

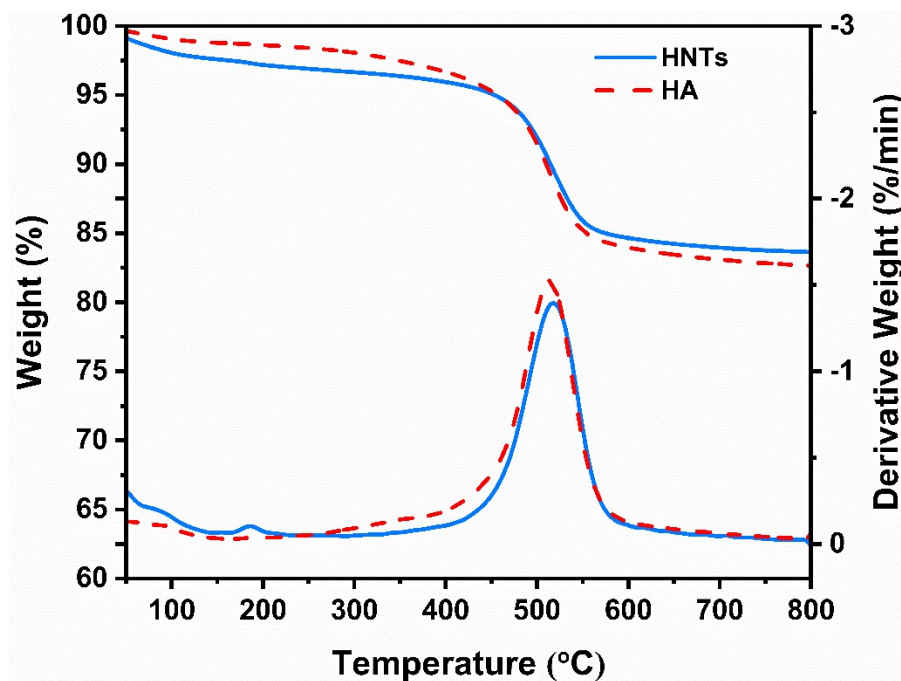


Figure S1. TGA and derivative thermogravimetric (DTG) curves of HNTs and HA.

Table S2. Weight losses of the HNTs and HA extracted from the TGA data.

Temperature range (°C)	% Weight loss	
	HNTs	HA
30–150	2.18	1.05
250–800	13.27	15.74
Grafting density (molecule/nm²)**	-	6.74

**The amount of APTES grafted onto the HNTs surface were calculated using the equation presented in our previous work.⁴⁶

(a)									
(b)									
	Pure HA	HA/TNT 10^{-4} M	HA/TNT 10^{-5} M	HA/TNT 10^{-6} M	HA/TNT 10^{-7} M	HA/TNT 10^{-8} M	HA/TNT 10^{-9} M	HA/TNT 10^{-10} M	HA/TNT 10^{-11} M

Figure S2. (a) A gradual change in color to the red color of a Meisenheimer complex after the addition of different concentrations of TNT solution into HA powder. (b) The HA/TNT mixture in powder form after solvent evaporation.

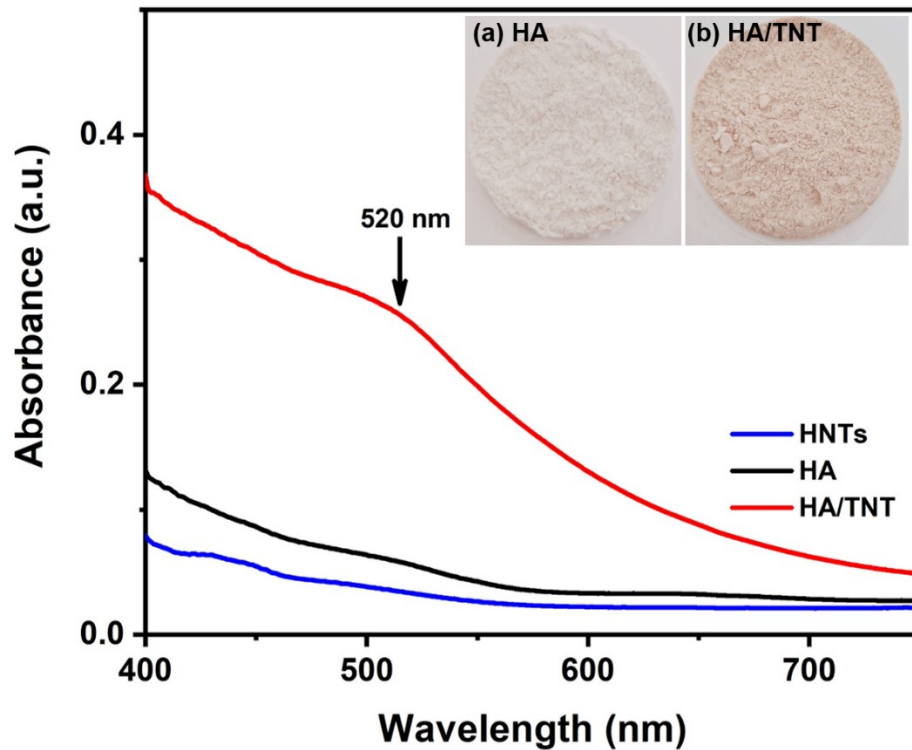


Figure S3. UV-vis absorption spectra of the powder samples of HNTs (blue line), HA (black line), and HA/TNT in the presence of 10^{-4} M TNT (red line). The inset shows the photos of the (a) HA and (b) HA/TNT powder samples captured by a mobile camera in daylight; the white color of the HA powder turns to red of a Meisenheimer complex of HA/TNT.

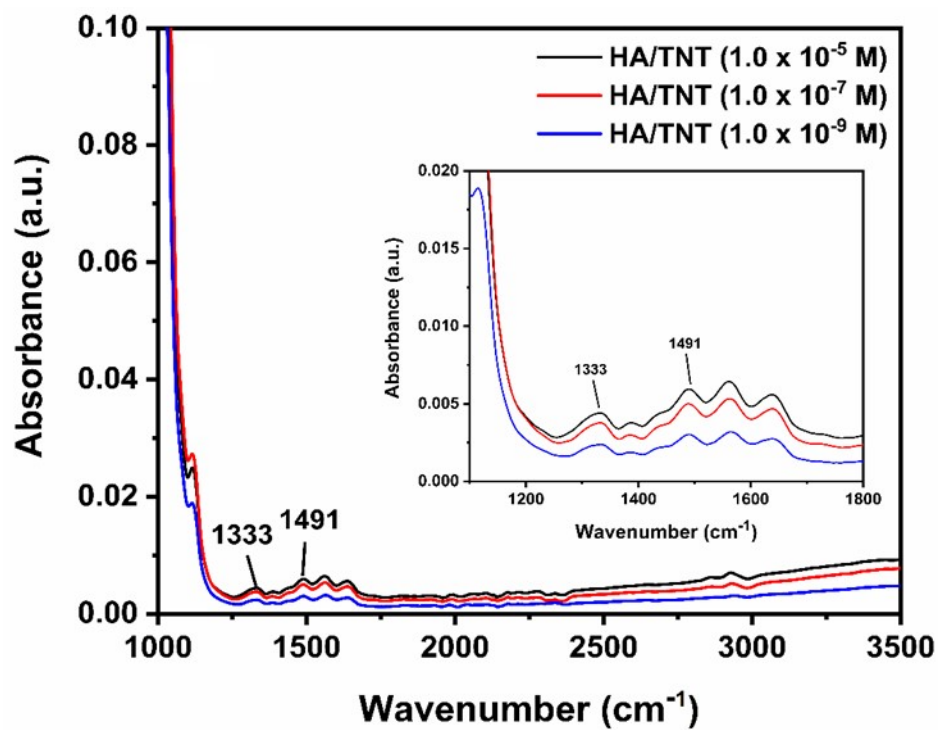


Figure S4. FTIR spectra of the powder products obtained from the reaction of APTES-modified HNTs (HA) and TNT at concentration of 1.0×10^{-9} M to 1.0×10^{-5} M. The baselines of all spectra were subtracted by the data of the pure HA.

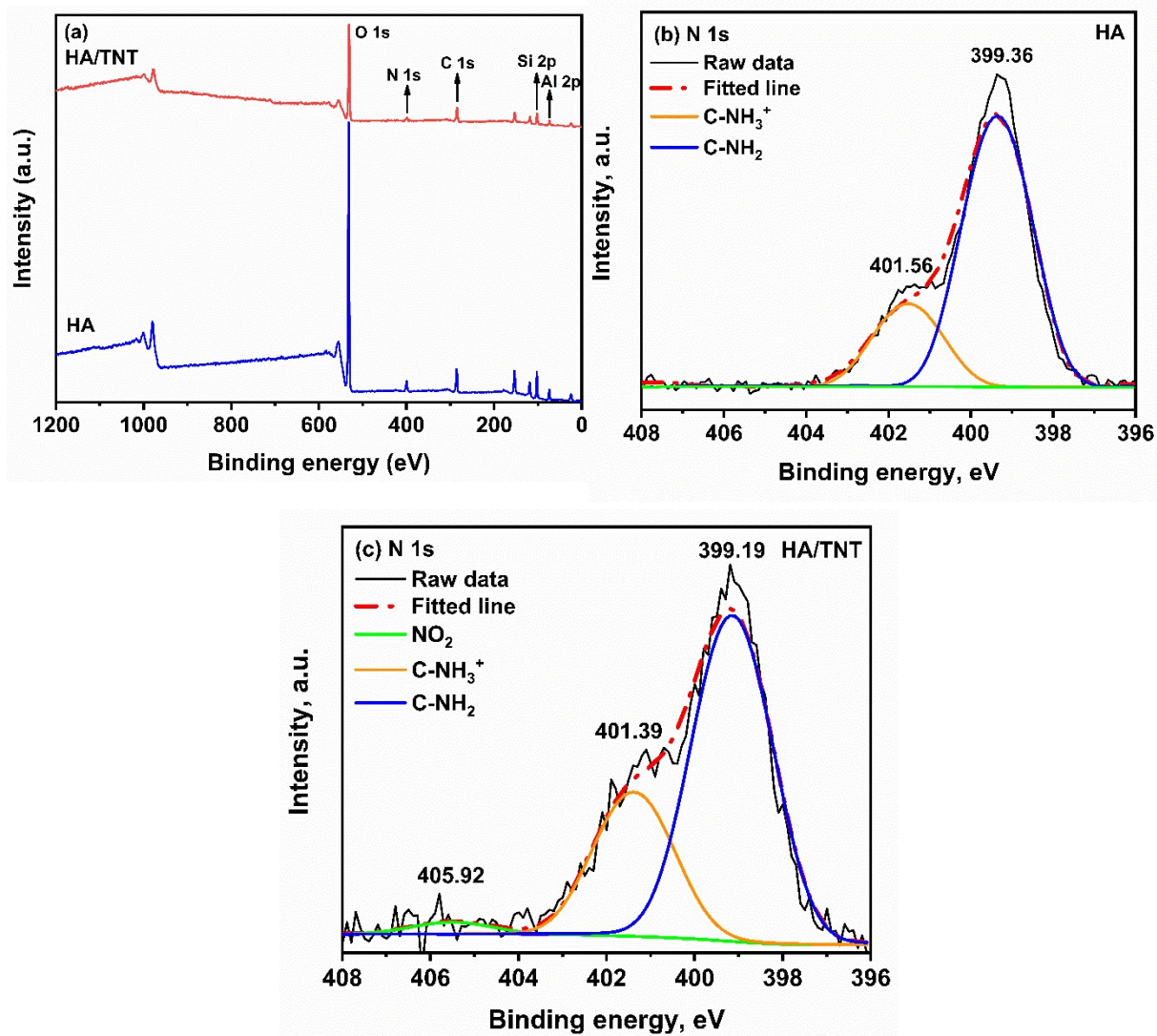


Figure S5. (a) Survey XPS spectra of the HA and HA/TNT with a TNT concentration of 10^{-4} M, and high resolution XPS spectra of N 1s in (a) the HA and (b) HA/TNT.

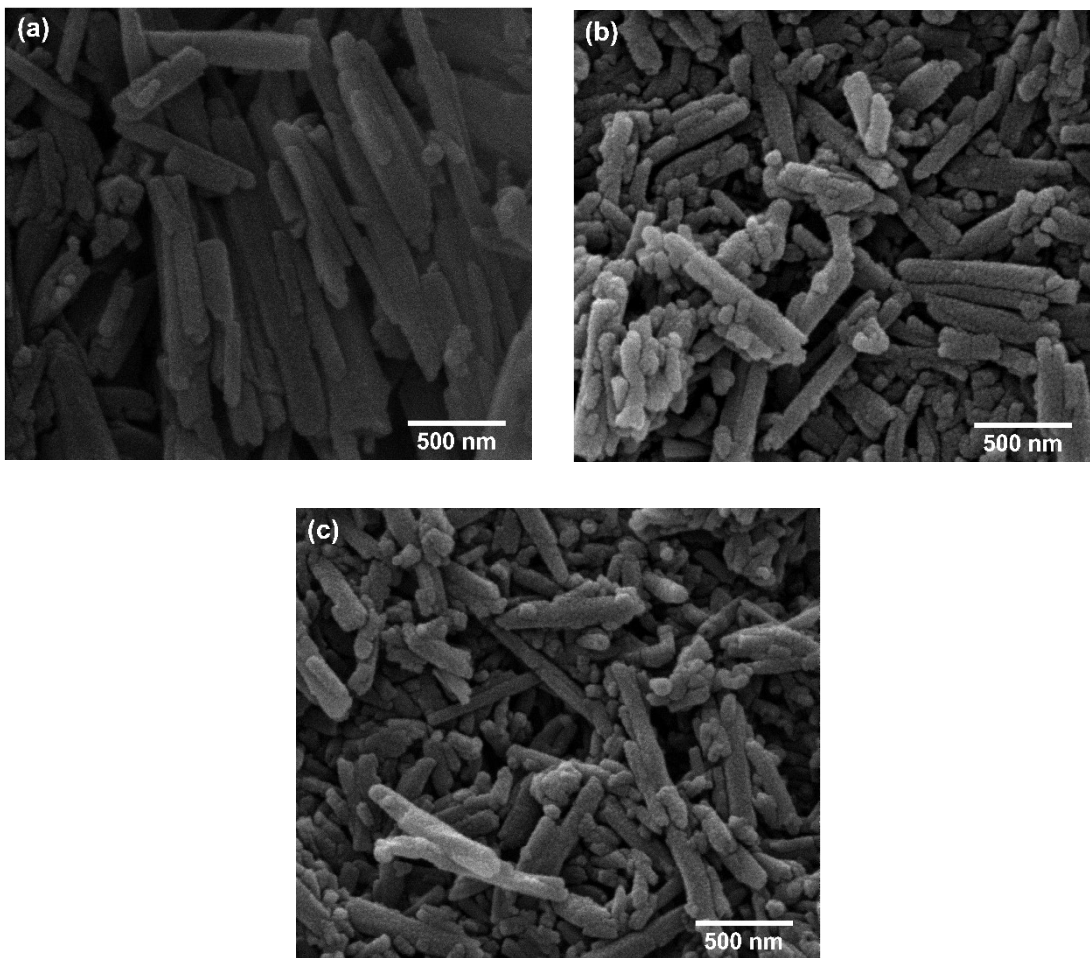


Figure S6. SEM images of (a) HNTs, (b) HA, and (c) HA/TNT with a TNT concentration of 10^{-4} M.

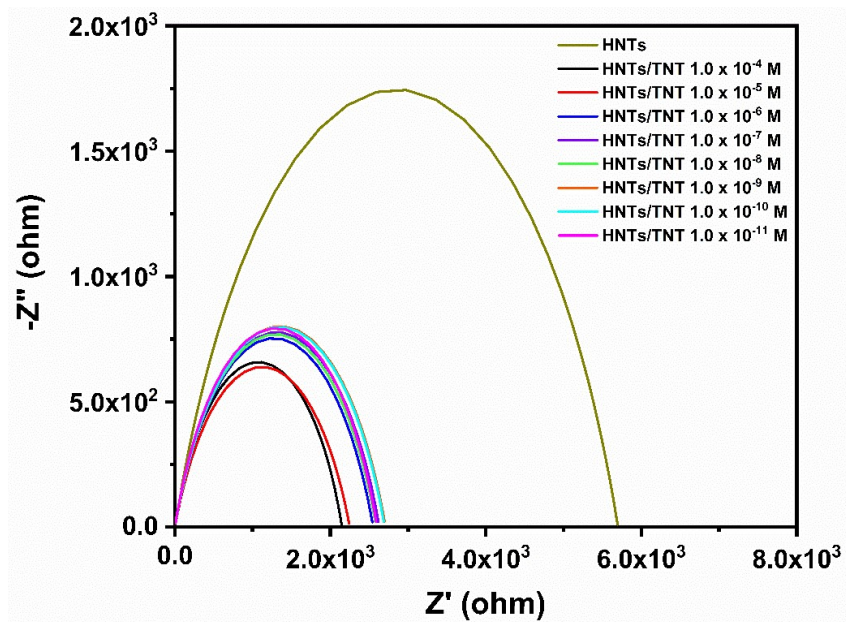


Figure S7. Nyquist plots of the bare HNTs and HNTs/TNT with presence of TNT in concentrations ranging from 1.0×10^{-11} M to 1.0×10^{-4} M. Z'' and Z' are the imaginary and real parts of impedance, respectively. The impedance data were fitted to a Randles circuit model and only the fitted data are shown as solid lines.

Table S3. Resistance (R) of the HA plate electrodes with various structurally-related nitroaromatics at a concentration of 1.0×10^{-6} M. Three replications of all the experiments were performed using the same batch of samples.

Material	Resistance (Ohm)		
	Replication	Mean	SD
HA (control experiment)	(1) 2.25E+07	2.22E+07	0.03E+07
	(2) 2.20E+07		
	(3) 2.20E+07		
TNT	(1) 0.54E+07	0.53E+07	0.02E+07
	(2) 0.54E+07		
	(3) 0.50E+07		
4-NP	(1) 1.11E+07	1.19E+07	0.09E+07
	(2) 1.19E+07		
	(3) 1.29E+07		
2,4-DNP	(1) 1.38E+07	1.39E+07	0.06E+07
	(2) 1.46E+07		
	(3) 1.33E+07		
2,6-DNT	(1) 1.90E+07	1.97E+07	0.12E+07
	(2) 2.10E+07		
	(3) 1.90E+07		

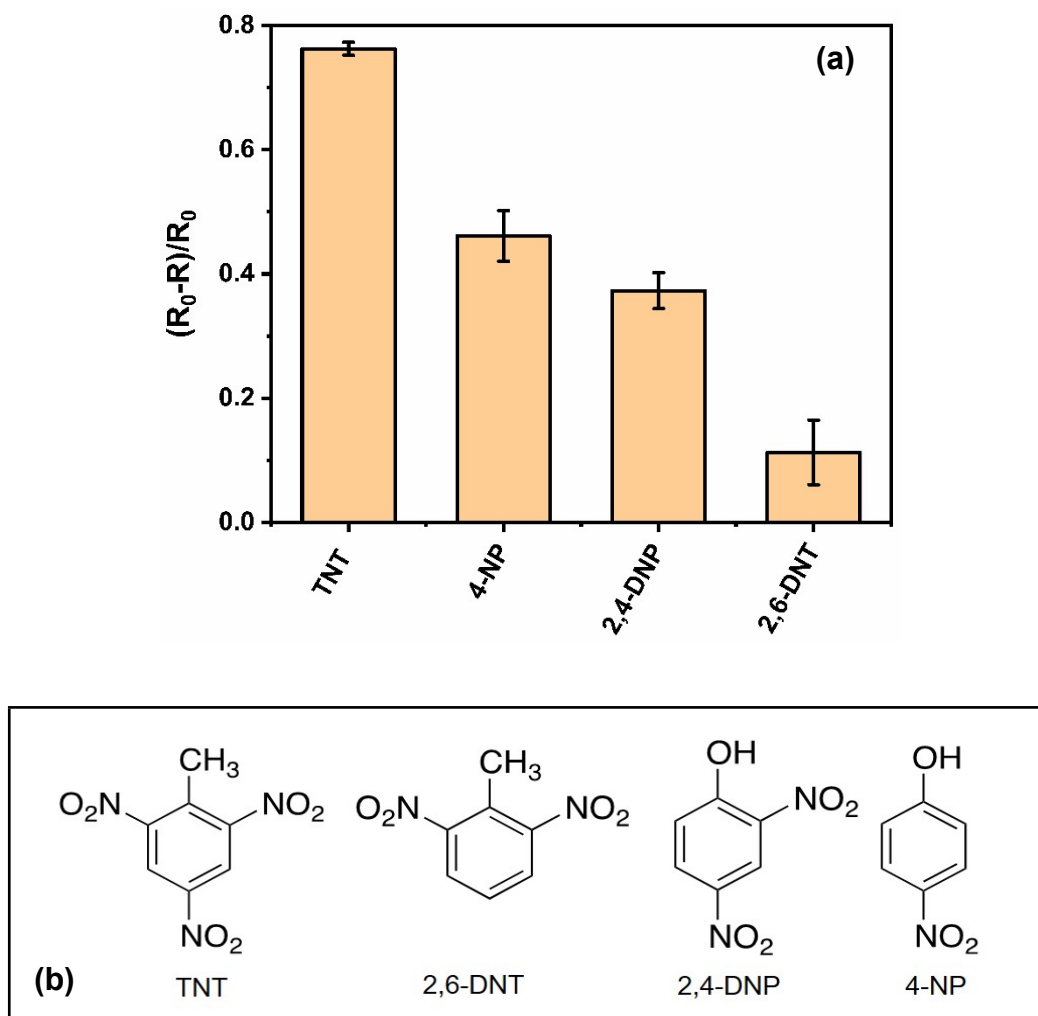


Figure S8. (a) Relative changes in the resistance of the HA plate electrodes with different nitroaromatics at a concentration of 1.0×10^{-6} M, where R_0 and R denote the resistance of the HA plate electrode measured without and with nitroaromatics, respectively. All experiments were conducted in three replications using the same batch of HA samples. (b) Chemical structures of the nitroaromatic compounds used in this study: TNT, 2,6-dinitrotoluene (2,6-DNT), 2,4-dinitrophenol (2,4-DNP), and 4-nitrophenol (4-NP).

Table S4. Resistance (R) of the HA plate electrodes recorded during the TNT-binding/removal cycles. The TNT-binding cycles were conducted with a TNT concentration of 1.0×10^{-6} M.

Three replications of all the experiments were performed using the same batch of samples.

Cycle	TNT removal			TNT binding		
	R (Ohm)	Mean	SD	R (Ohm)	Mean	SD
1	6.54E+07	6.48E+07	0.09E+07	5.52E+06	5.62E+06	0.13E+06
	6.53E+07			5.77E+06		
	6.37E+07			5.56E+06		
2	6.21E+07	6.10E+07	0.12E+07	5.77E+06	5.65E+06	0.20E+06
	6.11E+07			5.42E+06		
	5.98E+07			5.78E+06		
3	5.99E+07	5.95E+07	0.05E+07	5.40E+06	5.34E+06	0.15E+06
	5.89E+07			5.17E+06		
	5.98E+07			5.45E+06		
4	5.84E+07	5.76E+07	0.07E+07	5.34E+06	5.35E+06	0.26E+06
	5.74E+07			5.09E+06		
	5.70E+07			5.61E+06		
5	6.09E+07	6.25E+07	0.16E+07	5.18E+06	5.35E+06	0.16E+06
	6.25E+07			5.51E+06		
	6.41E+07			5.36E+06		